Neoplasia 69 (2025) 101229

Contents lists available at ScienceDirect

Neoplasia

journal homepage: www.elsevier.com/locate/neo

Original Research

Proteomic analysis uncovers biological diversity in molecularly defined endometrial carcinomas

Dawn R. Cochrane [a,b,1,*], Gian Luca Negri [c,1], Jutta Huvila [d], Forouh Kalantari [e], David A. Farnell [f], Nissreen Mohammad [f], Emily Thompson [f], Winnie Yang [a], Amy Lum [a], Sandra E. Spencer [c], Ryan Riley [c], Amy Jamieson [b], Samuel Leung [g], Derek Chiu [g], Christine Chow [g], Jamie L.P. Lim [a], Martin Köbel [h], Stefan Kommoss [i], Friedrich Kommoss [j], Blake Gilks [e,f], Lien Hoang [e,f], David G. Huntsman [a,b,e,g,h], Gregg B. Morin [k,c], Jessica N. McAlpine [b]

[a] Department of Molecular Oncology, BC Cancer Research Institute, Vancouver, BC, Canada
[b] Department of Gynecology and Obstetrics, University of British Columbia, Vancouver, BC, Canada
[c] Michael Smith Genome Sciences Centre, BC Cancer Research Institute, Vancouver, BC, Canada
[d] University of Turku, Turku University Hospital, Turku, Finland
[e] Department of Pathology and Laboratory Medicine, University of British Columbia, Vancouver, BC, Canada
[f] Department of Anatomical Pathology, Vancouver General Hospital, Vancouver, BC, Canada
[g] Molecular and Advanced Pathology Core, University of British Columbia, Vancouver, BC, Canada
[h] Department of Pathology and Laboratory Medicine, University of Calgary, Calgary, AB, Canada
[i] Department of Obstetrics and Gynecology, University of Tübingen, Germany
[j] Institute of Pathology, Medizin Campus Bodensee, Friedrichshafen, Germany
[k] Department of Molecular Genetics, University of British Columbia, Vancouver, BC, Canada

ARTICLE INFO

Keywords:
Endometrial carcinoma
Molecular subtype
Proteomics

ABSTRACT

While endometrial cancer has an overall favorable prognosis, some patients have poor outcomes and may benefit from further refinements of the current classification systems. Molecular classification stratifies endometrial cancer patients into four prognostic subtypes: *POLE*mut, MMRd (mismatch repair deficient), p53abn, and NSMP (no specific molecular profile), where patients with *POLE*mut have the best prognosis and p53abn has the worst prognosis. We used proteomic profiling to assess if additional prognostic or predictive information could be identified across or within molecular subtypes. Global proteome profiling of formalin fixed, paraffin embedded samples, that had clinicopathologic and outcome data, was performed on 184 endometrial cancers encompassing all four molecular subtypes, including replicate samples of the same tumor, and both biopsy and final hysterectomy specimens. To ensure representation of each subtype, we profiled an approximately equal distribution in the 148 unique tumors; 34 (23%) *POLE*mut, 40 (27%) MMRd, 35 (24%) p53abn and 39 (26%) NSMP, rather than the population-based distributions. There was high reproducibility in the proteomic profiles of intra-tumor replicate samples, and between matched biopsy and hysterectomy tumor samples. Consensus clustering identified four clusters with different prognosis, named 'Adhesion', 'Immune', 'Proliferation', and 'Metabolic' based on the functional characteristics of the enriched proteins. We associated protein expression features with common mutations, molecular subtype, and outcomes. These results demonstrate the biologic diversity within endometrial cancers, both between and within molecular subtypes, and provide candidate features for functional and clinical investigation.

* Corresponding author at: Department of Molecular Oncology, BC Cancer Research Institute, Vancouver, BC, Canada.
E-mail address: dcochrane@bccrc.ca (D.R. Cochrane).
[1] These authors contributed equally to this work.

https://doi.org/10.1016/j.neo.2025.101229
Received 15 May 2025; Received in revised form 8 September 2025; Accepted 9 September 2025
Available online 17 September 2025

Introduction

Endometrial cancers are the most common gynecologic malignancy in North America. While the majority of endometrial cancers are associated with excellent five-year survival, approximately 20% of patients with endometrial cancer recur and ultimately die from their disease. The Cancer Genome Atlas (TCGA)-inspired pragmatic molecular classification of endometrial cancer has transformed categorization and risk group assignment of endometrial cancers [1–4]. Using a combination of focused sequencing and immunohistochemistry (IHC) four molecular subtypes have been identified; *POLE*mut (with pathogenic mutations in the exonuclease domain of polymerase epsilon), mismatch repair deficient (MMRd; with loss of one or more mismatch repair proteins, displaying microsatellite instability), p53 abnormal (p53abn; with either complete loss or overexpression of p53 proteins), and no specific molecular profile (NSMP; having none of these other specific features) [5–9]. Prognosis ranges from highly favourable (>95% 5-year survival) for patients with *POLE*mut tumors to very poor prognosis for patients with p53abn endometrial cancer, where over half of patients recur and die from their disease [10]. Additional predictive implications of molecular subtype assignment have also become apparent, including de-escalation of therapy for *POLE*mut cancers [11], and immune checkpoint inhibitors (ICI) for MMRd tumors [12,13].

Proteome profiling has been used to discover the biological underpinnings of various cancers such as altered metabolism in hepatocellular carcinoma [14,15] and clear cell ovarian carcinoma [16], or the immune microenvironment of head and neck cancers [17]. Further stratification of existing cancer subtypes, for example subtypes within triple negative breast cancers have been discovered using proteomic analysis [18,19]. Prognostic biomarkers, identifying patients more likely to relapse predict relapse [20], or predictive biomarkers, identifying patients more likely to respond to therapy [21] have been found using global proteomic profiling.

Within the framework of molecular classification of endometrial carcinomas, there is tremendous interest in further refining prognosis or providing greater precision in treatment selection. Our objective was to determine the value of proteomic assessment of endometrial cancers, across and within the landscape of the 4 molecular subtypes and to assess the feasibility of proteomic stratification from first diagnostic biopsy. Our large scale proteomic analysis of the four endometrial cancer molecular subtypes using patient hysterectomy and biopsy material provides a rich resource that associates biological features for a cohort of molecularly defined endometrial cancers with associated clinical characteristics and outcomes data.

Methods and materials

Cohort description

Following institutional review board approval, we identified a cohort of endometrial cancers that had previously undergone molecular classification and with complete clinicopathologic data and outcomes. A total of 184 individual formalin-fixed paraffin embedded (FFPE) samples extracted for proteomics, from 150 individual cases. Two samples were removed from the subtype analysis because one had insufficient proteomics signal and the other was reclassified as an ovarian tumor. The remaining 182 samples in the study consisted of 159 hysterectomies and 23 endometrial biopsies (obtained from office pipelle/sample or curettage). For subtype analysis, we used the hysterectomy proteomic data only (n=148). To examine technical reproducibility, we included 11 replicate hysterectomy samples, defined as being from a different tumor block of the same case. To compare hysterectomy to biopsy, we included 21 biopsy samples which were matched to hysterectomy samples. The final cohort (n=148) used for subtype analysis contained 34 *POLE*mut, 40 MMRd, 35 p53abn, and 39 NSMP. The cohort was designed to contain a balanced number of each molecular subtype, rather than the distribution within the population. 10μM scrolls to a total of 5cm^2 of tumor area were taken of each tumor, with macrodissection performed when necessary to ensure high tumor content.

Protein isolation, reduction, and alkylation, FFPE tissue

Tubes containing 10 μM slices of tissue were centrifuged for 1 min at 20,000 x g. Xylenes (800 μL, CAT #214736) was added to each tube, gently pipette mixed, and incubated for 5 min to deparaffinize the sample. Samples were centrifuged for 1 min at 20,000 x g and the supernatant discarded, then washed with an additional 800 μL of xylenes. 100 μL of lysis buffer (500 mM Tris-Cl pH 8, (CAT#C4706, Sigma), 2% w/v sodium dodecyl sulfate (Bio-Rad, CAT#1610302), 1% v/v NP40 (CAT#492016-100ML, Merck Millipore), 1% v/v Triton X100 (CAT#T8787, Sigma), 5 mM EDTA (Thermo Fisher, CAT#15575020), 50 mM sodium chloride (CAT#S7653, Sigma), 10 mM tris(2-carboxyethyl)phosphine hydrochloride, 40 mM chloroacetamide (in HPLC water) was added to the sample and the solution was heated at 95°C for 90 min with mixing at 1000 rpm. Tubes were cooled to room temperature prior to sample cleanup using the single pot solid phase enhanced sample preparation (SP3) method [22].

SP3 sample cleanup

SP3 was adapted from the published method [22]. Specifically, Sera-Mag SP3 1:1 bead mix (Sera-Mag Speed Beads, GE Life Sciences, CAT#45152105050350 and CAT#65152105050350) was rinsed once with HPLC water and diluted to a final working concentration of 20 μg/μL. 200 μg of this bead mixture was added to the entire FFPE sample and mixed by pipetting to generate a homogeneous solution. To induce protein binding to the beads, ethanol (Sigma, CAT#34852) was added to achieve a final concentration of 50% (v/v). Bead-protein solutions were pipette mixed to ensure a homogeneous distribution of the beads and incubated for 5 min at room temperature. After incubation, tubes were placed on a magnetic rack for 1 min and the supernatant was removed and discarded. The beads were rinsed three times with 200 μL of 80% ethanol, and the supernatant was discarded. Rinsed beads were reconstituted in 100 μL 0.2 M HEPES pH 8 containing 2 μg trypsin/rLysC mix (Promega, CAT#V5071), and pipette mixed. Mixtures were incubated overnight (14+ hours) at 37°C in a thermomixer (Eppendorf, CAT#05-400-205). The supernatants were recovered using a magnetic rack and transferred to fresh 1.5 mL polypropylene Eppendorf tubes with a snap-lock lid (Eppendorf, CAT#022363204). Samples were stored at -80°C and 10% of the resulting peptide mixture was used for QC of the sample prior to labeling.

TMT labeling

TMT 11-plex labeling kits were obtained from Pierce (CAT#A34808). Each TMT label (5 mg per vial) was reconstituted in 500 μL of acetonitrile and frozen at -80°C. Prior to labeling, TMT labels were removed from the freezer and allowed to equilibrate at room temperature. TMT label was added to the peptide sample in two volumetrically equal steps of 10 μL (100 μg), 30 min apart at room temperature. Reactions were quenched by addition of 10 μL of 1 M glycine (CAT#G8898, Sigma). Labeled peptides were concentrated in a Labconco centrivap concentrator (CAT#781001010234) with a Thermo-Savant RVT400 refrigerated vapor trap (CAT#RVT400-230) to remove acetonitrile, and the differentially labeled peptides were combined. All samples were labeled with one of 11 TMT labels and batched prior to mass spectrometry. Batches contained 8 tumor samples, one SuperMix control (a mixture of lysates of 13 common cancer cell lines [19], a pooled all sample control (PIS; pooled internal standard), and another sample pool that was not used in the analysis. TMT channel assignments for the 23 plexes are described in Supplemental Table 1. The control channels increased the likelihood that the same peptides would be

detected in all batches and were utilized in normalization of the data between batches.

SepPak clean-up

SepPak C18, 50 mg columns were purchased from Waters (CAT#-WAT054960). TMT labeled samples were acidified with trifluoroacetic acid (Sigma, CAT#T6508-100ML) to a final concentration of 1%. Columns were washed with two aliquots of 1 mL 0.1% trifluoroacetic acid in HPLC grade acetonitrile (Sigma, CAT#34851) and conditioned using two aliquots of 1 mL 0.1% trifluoroacetic acid in HPLC grade water. Samples were loaded and rinsed with three aliquots of 1 mL of 0.1% formic acid (Sigma, CAT#33015) in HPLC grade water and peptides were eluted using two aliquots of 600 µL 0.1% formic acid in 20%/80% HPLC water/HPLC acetonitrile. Sample volume was reduced to less than 200 µL by vacuum centrifugation.

HPLC fractionation

High-pH reversed phase separation was performed on an Agilent 1100 HPLC system equipped with a diode array detector (254, 260, and 280 nm). Fractionation was performed on a Kinetix EVO C18 column (2.1 x 150 mm, 1.7 µm core shell, 100Å, Phenomenex). Elution was performed at a flow rate of 0.25 mL/min using a gradient of mobile phase A (10 mM ammonium bicarbonate, pH 8) and B (acetonitrile), from 3% to 35% over 60 min. Fractions were collected every minute across the elution window (8-52 min) for a total of 48 fractions which were concatenated to 12 final fractions (e.g. 1 + 13 + 25 + 37 = fraction 1; 2 + 14 + 26 + 38 = fraction 2, etc). Fractions were dried in a vacuum centrifuge and reconstituted in 0.1% formic acid HPLC water prior to mass spectrometry analysis.

Mass spectrometry (MS) analysis

Analysis of peptide fractions was carried out on an Orbitrap Fusion Tribrid MS platform (Thermo Scientific). Samples were introduced using an Easy-nLC 1000 system (Thermo Scientific). Columns used for trapping and separations were packed in-house. Trapping columns were packed in 100 µm internal diameter capillaries to a length of 2.5-5 mm with C18 beads (Reprosil-Pur, Dr. Maisch, 3 µm particle size). Trapping was carried out for a total volume of 10 µL at a flow of 25 µL/min. After trapping, gradient elution of peptides was performed on a C18 (Reprosil-Pur, Dr. Maisch, 3 µm particle size) column packed in-house to a length of 25 cm in 100 µm internal diameter capillaries with a laser-pulled and fritted electrospray tip. Elution was performed at a flow rate of 450 nL/min. Mobile phase B (HPLC acetonitrile and 0.1% formic acid) was increased from 3-7% in mobile phase A (water and 0.1% formic acid) over 2 min, to 25% B over 94 min, to 40% B over 17 min, then a 1 min increase to 80% and the column was washed for 6 min.

Data acquisition on the ThermoFisher Orbitrap Fusion was carried out using a data-dependent method. MS1 survey scans in positive ion mode covering the normal mass range of 350 – 1200 were acquired at a resolution of 120,000 (at m/z 200), with quadrupole isolation enabled, an S-Lens RF Level of 60%, a maximum fill time of 100 ms, a single microscan, and an automatic gain control (AGC) target value of 4e5. For MS2 scan triggering, peptide monoisotopic precursor selection was enabled, charge state filtering was limited to 2 – 6 and undetermined charge states were included and charge states of 25 and higher were excluded. Dynamic exclusion of previously selected masses after 1 observation was enabled for 60 s with a tolerance of 20 ppm. MS2 scans were acquired in the Orbitrap normal scan range mode at a resolution of 50,000 with a starting mass of 120 after HCD fragmentation. A maximum fill time of 86 ms, quadrupole isolation, isolation offset off, an isolation window of 1.4 m/z, fixed collision energy of 40%, injection for all available parallelizable time turned OFF, and an AGC target value of 1.2e5. The total allowable cycle time was set to 3 s. MS1 scans were acquired in profile mode, and MS2 in centroid format.

Data processing of mass spectrometry data

Raw MS data were searched using Sequest HT algorithm through Proteome Discoverer suite (v2.4) (Thermo Scientific), against a human reference (2018/08/03 Swissprot; 20,369 sequences). Precursor and fragment mass tolerance were set at 10 ppm and 0.05 Da, respectively. Dynamic modifications included Oxidation (15.995 Da, M), Acetylation (42.011 Da, N-Term), Methylation (14.016 Da,K) and TMT (229.163 Da, K). Static modification included Carbamidomethyl (57.021 Da, C), and TMT (229.163 Da, N-Term). Peptide-to-spectrum matches (PSM) were filtered using Percolator by searching the results against a decoy sequence set, only PSMs with FDR < 1% were retained in the downstream analysis. PSMs were further filtered out if they had a signal-to-noise ratio (S/N) lower than 10 in the PIS channel and if they mapped to more than one unique protein. To normalize input signal, channel total intensity was scaled to 1e08. Each S/N was normalized to PIS channel (ratio) and, for each peptide, the median ratio of the 3 PSMs with the lowest isolation interference was used. Peptides were then median-aggregated to the protein level. Proteins with fewer than two identified peptides were excluded from analysis in the global proteome data. To estimate protein relative abundance, the S/N sum of the 3 highest abundance PSMs was taken and the average across channel was multiplied to S/N protein ratios obtained previously.

Differential protein expression analysis was performed with Differential Expression analysis of quantitative Mass Spectrometry data (DEqMS) R package [23]. Gene set enrichment analysis on differential expression was performed on the pre-ranked t-statistic with the R package fgsea [24] (minSize = 2,maxSize = 500), using the GO term signature derived from the Molecular Signature Database (MSigDB) [25]. Samples were clustered by selecting proteins that were quantified in all samples and that showed the highest variability (top 25% median absolute deviation) across the cohort. ConsensusClusterPlus R package [26,27] was used with the following parameters (maxK = 8, clusterAlg = 'km',distance = 'euclidean',reps = 3000, seed = 3326). The number of final clusters used was determined based on inspection of consensus matrix and examining the change in consensus cumulative distribution function area with delta plots. The "survminer" and "survival" R packages were used to conduct statistical survival analysis.

A previously published endometrial carcinoma cohort [28] was used to identify commonalities and disparities in the differential protein expression analysis between genomic subtypes and between endometrioid and serous histotypes. Data were downloaded from Proteomic Data Commons (PDC) [29] and the log2 transformed protein abundance relative to a reference ("Unshared Log Ratio") was used for downstream analysis with DEqMS as above.

Data availability

The mass spectrometry proteomics data have been deposited to the ProteomeXchange Consortium via the PRIDE [30] partner repository with the dataset identifier PXD057700.

Additional methods for immunohistochemistry, organoid culture, CRISPR-Cas9 knockouts, and western blotting can be found in Supplemental Methods and Materials.

Results

Proteomics cohort description

Global proteome profiling using the clinical SP3-CTP workflow [22] was performed on 184 tumor samples. Two samples were removed from the final analysis; one sample lacking sufficient proteomics signal and one that was reclassified as an ovarian carcinoma, leaving 182 endometrial carcinoma samples included in the study (Fig. 1A, Supplemental

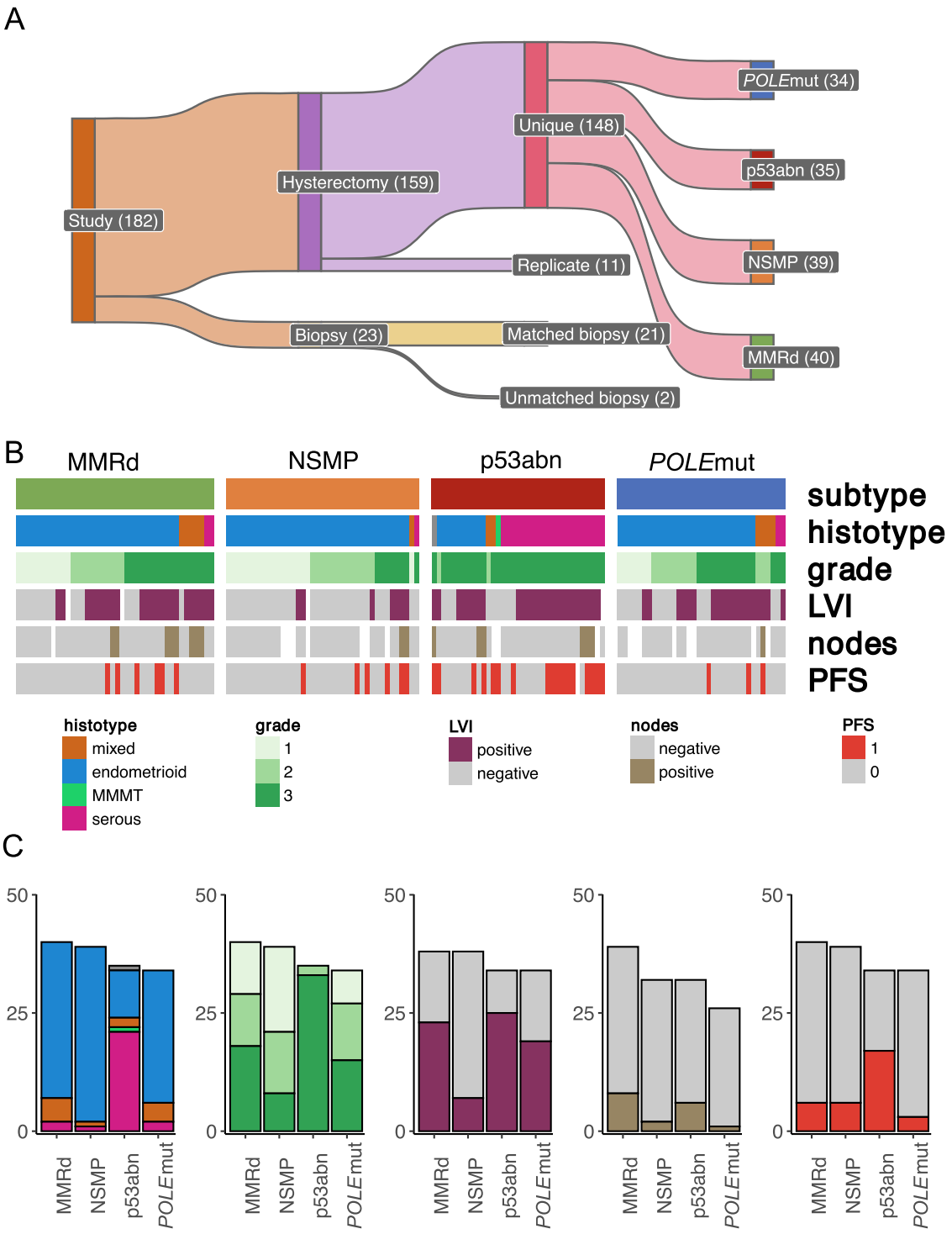

Fig. 1. Cohort Description. A. Schematic of proteomic workflow depicting the number of samples across the 4 molecular cohorts. Of the 182 samples in the study, 159 were hysterectomies and 23 were biopsies. The study included 11 replicate hysterectomy samples, defined as being from a different tumor block of the same case. There were 21 biopsy samples which were matched to hysterectomy samples and 2 biopsies that were not matched to hysterectomy. For subtype analysis, the proteomic data from 148 hysterectomy samples was used, consisting of 34 *POLE*mut, 40 MMRd, 35 p53abn, and 39 NSMP. The cohort features including histotype, grade, lymphovascular invasion (LVI), lymph node positivity and progression free survival (PFS) are displayed for individual samples (**B**) and as bar plots (**C**). PFS of 1 indicates a progression event within 5 years, while 0 indicates no progression event. MMMT indicates malignant mixed Mullerian tumor.

Table 1). Proteomics was performed on 159 hysterectomy samples obtained from 148 patients. There were 11 replicate hysterectomy samples, representing different regions of the endometrial tumor. A total of 23 endometrial carcinoma biopsy samples were also assessed, with 21 of these having matched hysterectomy samples.

Our cohort had approximately equal distribution of the 4 molecular subtypes; 34 (23%) *POLE*mut, 40 (27%) MMRd, 35 (24%) p53abn and 39 (26%) NSMP endometrial cancers (Fig. 1B, Supplemental Table 2). The clinicopathologic features of the cohort are summarized in Fig. 1B and C, and detailed in Supplemental Table 2. The majority of p53abn

endometrial cancers were grade 3 endometrioid, serous and carcinosarcoma (MMMT) histotypes, whereas the endometrioid histotype was predominant in the other molecular subtypes (Fig. 1B, C). The greatest number of disease progression events within 5 years was observed in patients with p53abn endometrial cancers (Fig. 1B, C). Lymphovascular space invasion (LVI) was observed less frequently in the NSMP subtype (Fig. 1B, C and Supplemental Table 1).

In total, we quantified 6089 proteins, with a minimum coverage of 2 peptides, one of which was unique, with 3706 proteins quantified in each sample across the 23 TMT-11 batches. We tested for reproducibility between duplicate hysterectomy samples by analyzing the 11 biological replicate samples run, where a different tumor block from the same patient was sampled. The correlation between tumors sampled in different locations of the endometrium was very high, most having a Pearson correlation coefficient greater than 0.9, with the 3 lowest correlations (0.895, 0.905, 0.929) found within *POLE*mut cases, possibly reflecting tumor heterogeneity secondary to ultramutated phenotype (Fig. S1). Matched hysterectomy and biopsy samples were analyzed for 21 cases; the Pearson correlation coefficient was above 0.9 for all but one sample (Fig. S2A). Differential protein expression analysis between matched diagnostic biopsies and hysterectomies showed higher blood components (e.g. hemoglobin and fibrinogen proteins) in the biopsies and higher matrix proteins (e.g. collagens) in the hysterectomies (Fig. S2B). Removal of the blood and matrix proteins from the analysis increased the correlation between matched biopsy and hysterectomy in most of the samples by an average of 0.0043 (Fig. S2C).

Consensus clustering of proteomic data

Consensus clustering was performed on hysterectomy samples from 148 patients, resulting in four proteomic clusters (Fig. 2A). Pathway analysis (Fig. 2B) and differential protein expression (Fig. S3) was used to name the clusters. We named Cluster 1 the 'Adhesion' cluster, as it is enriched in proteins involved in actin, collagen, and integrin binding. Cluster 2 is named the 'Immune' cluster because it is enriched in proteins in the pathway for leukocyte activation. Cluster 3 is enriched in pathways involved DNA replication, transcription and translation and is called the 'Proliferation' cluster. Cluster 4 is named the 'Metabolic' cluster, as it is enriched for some metabolic processes. The breakdown of the stage, histotype, and molecular subtype for each proteomic cluster is shown in Fig. S4. Cluster 1 is predominantly endometrioid and low stage with a mixture of molecular subtypes, but a higher proportion of *POLE*mut tumors than in the other clusters. Cluster 2 has more serous cases than cluster 1, mostly low stage and a mixture of molecular subtypes. Cluster 3 is enriched for high stage, p53abn and serous histotypes. Cluster 4 is almost exclusively endometrioid, with the lowest proportion of high stage cases and predominantly MMRd and NSMP. The clusters have different survival characteristics with the Proliferation Cluster (Cluster 3) having the worst prognosis and the Immune Cluster (Cluster 2) having the best prognosis for both overall and disease specific survival (Fig. 2C). The Adhesion (Cluster 1) and Metabolic (Cluster 4) clusters have intermediate survival.

Differential protein expression between molecular subtypes

Protein expression was compared between the four ProMisE molecular subtypes (Figs. 3A, S5A). p53 protein was more highly expressed in the p53abn group compared to the other groups (Fig. 3A, B). Other proteins that have been previously shown to be associated with aggressive clinical course or serous histomorphology were also enriched in the p53abn endometrial cancers, including UCHL1, L1RE1 (LINE-1), ISG15, and IGF2BP3 [31–37]. Growth factor receptor bound protein 7 (GRB7), was also found to be more highly expressed in p53abn tumors (Fig. 3A, D). IHC for GRB7 confirmed high protein levels in p53abn compared to other subgroups, with more tumors displaying high intensity staining (Fig. 3D), percent positive tumor cells and a higher H-score (Fig. S6). The gene encoding GRB7 is adjacent to *ERBB2* on chromosome 7 and these genes are often co-amplified [38–42]. Using IHC, we found only a weak correlation between GRB7 and HER2 expression (Fig. S6B), suggesting that only a subset of GRB7 positive tumors have genomic amplifications encompassing the *ERBB2* and *GRB7* loci. In some cases, the focal staining positivity of HER2 and GRB7 expression were matched, suggesting genomic co-amplification in these tumors (Fig. S6C). High GRB7 is associated with worse disease specific survival (hazard ratio; HR=2.39, Fig. 3E) and progression free survival (HR=1.87, Fig. S6D) in the whole cohort, while there was no significant association of GRB7 with survival within the individual molecular subtypes (not shown).

Comparison with published proteomics dataset

We compared our proteomics dataset with a previously published dataset of 95 tumors, of which 7% were POLE ultramutated (*POLE*mut), 26% MSI hypermutated (MMRd), 21% CN-high (p53abn), and 45% CN-low (NSMP). When comparing the proteins enriched and depleted within each molecular subtype, we found good correlation between our proteomic data and this previous proteomic study [28], with the best correlation found in MMRd, p53abn, NSMP groups (all with $p<2.2e-16$, Fig. S5). In the ultramutated *POLE*mut tumors, genetic instability results in high intratumoral heterogeneity and there is less correlation between our study and previously published data ($p=0.00073$) [28]. As has been found previously [28], RPL22L1 is enriched in the MMRd group compared to the others (Fig. S5B). In the MMRd subtype, there is an abundance of proteins involved in steroid signaling such as PDIA2, SCGB2A1, and SCGB1D2 [43–45], and cell adhesion and polarity such as PATJ, CEACAM5, and LAD1 [46–48]. The NSMP group is enriched in keratins (KRT5, KRT6A, and KRT75) and metabolic proteins that have previously been implicated in cancer such as ASRGL1, DPEP1, and ACSL5 [49–51]. Interestingly, we found no correlation for proteins upregulated in the *POLE*mut subtype except for HLA and linker Histone H1.1 proteins [52].

Comparison of protein expression between endometrioid and serous histotype in our cohort showed an enrichment for many proteins that have been previously associated with serous or p53abn endometrial cancers, including UCHL1, HMGA1, IGF2BP3, P53, and L1RE1 (Fig. S7A). The endometrioid tumors were enriched for proteins such as PIGR, ASRGL1, and HGD (Fig. S7A). We compared our results with those in the Dou et al. proteomic study which had also performed a comparison of serous and non-serous tumors [28] and found good correlation (Pearson's $R = 0.63$) between the two studies (Fig. S7B).

Protein expression in relation to ARID1A status

ARID1A mutations, leading to a loss of ARID1A protein expression, are found in 18-60% of endometrial cancers, depending on grade and histotype [53–55]. ARID1A status was determined by IHC for all samples in the cohort. In tumors that express ARID1A, there was an increase in proteins involved in the retinoic acid pathway (RBP1, CRABP2, ADH1B, and ALDH1A2) and in the ARID1A negative tumors an enrichment for proteins related to anti-microbial response (SLP1, LYZ, CAMP, DPP4, GBP1, GBP2, GBP5, RNASE3, BPI, and CYBA), and specifically proteins related to neutrophils (MPO, CTSG, AZU1, and LCN2) (Fig. 4A). IHC was performed for ARID1A, RBP1, CRABP2, and MPO confirming that ARID1A positive tumors tend to express RBP1 and CRABP2, while ARID1A negative express MPO (Fig. 4B). The Spearman's correlations between ARID1A expression and RBP1 was 0.22 ($p=0.0065$), 0.28 ($p=0.00045$) between ARID1A and CRABP2, and 0.21 ($p=0.01$) between ARID1A and MPO (Fig. S8). We found a positive correlation between RBP1 and ARID1A by western blot in endometrial and clear cell ovarian cancer cell lines (Fig. S9A). In isogenic lines where ARID1A has been depleted using CRISPR-Cas9, RBP1 levels were decreased (Fig. S9B). Similarly, in organoids we derived from normal endometrial

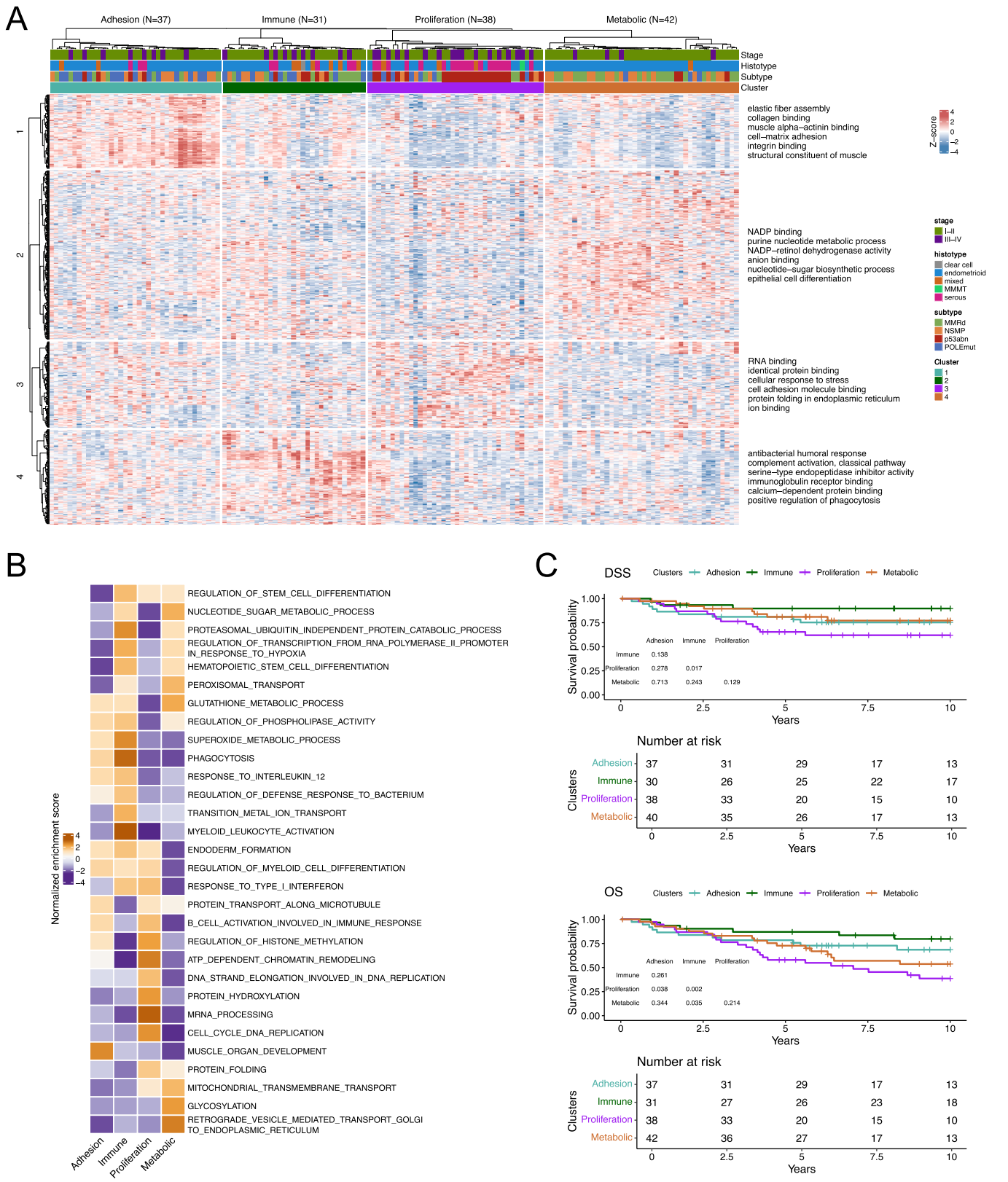

Fig. 2. Clustering of the proteomic data. A. Heatmap of consensus clustering of the top 25% most variable proteins (N = 927) resulting in four clusters. The histotype, molecular subtype, and stage are shown above. **B.** Heatmap showing the Normalized Enrichment Score of pathways associated with each of the four clusters. The clusters were renamed based on gene and pathway enrichment as Adhesion (Cluster 1), Immune (Cluster 2), Proliferation (Cluster 3), and Metabolic (Cluster 4). **C.** Kaplan-Meier survival curves are shown for the four clusters, disease specific survival (DSS, top) and overall survival (OS, bottom). The p-value for each pair of clusters is shown at the bottom left of the plots.

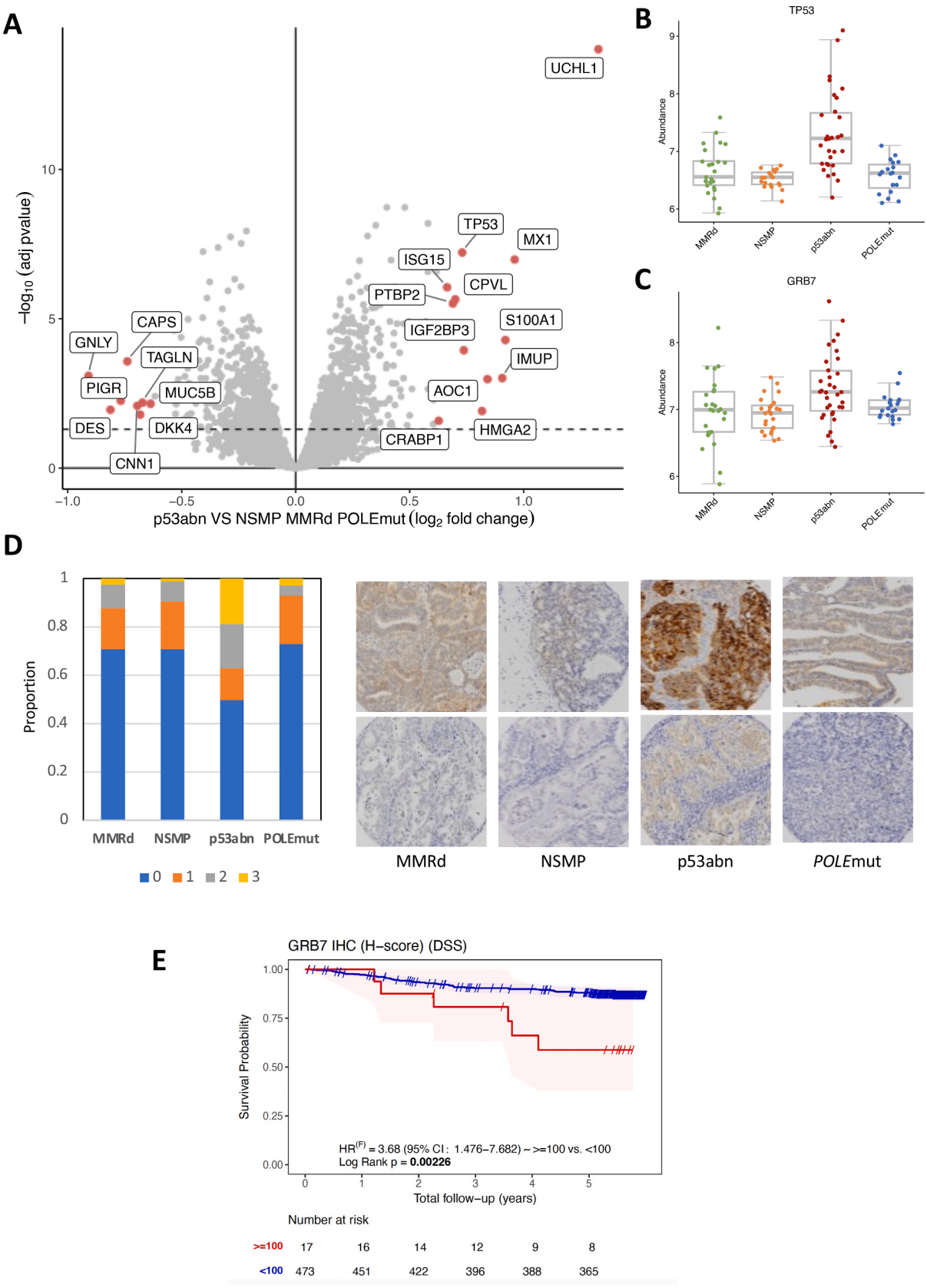

Fig. 3. Differential protein expression among molecular subtypes. A. Volcano plot comparing protein expression between p53abn (right) and the other molecular subtypes (left). **B.** Protein abundance of p53 measured from proteomics among the four molecular subtypes. **C.** Protein abundance of Grb7 among the molecular subtypes. **D.** Endometrial tumor TMA (16-005, 475 cases) was immunostained for Grb7 and intensity scored as 0 (negative), 1 (weak), 2 (moderate) and 3 (strong). Proportion of the different intensities of Grb7 staining among the molecular subtypes and representative image of staining (20X magnification). **E.** Kaplan-Meier survival curve for disease specific survival for Grb7 H-score (calculated by multiplying intensity by percent positive staining) in all molecular subtypes.

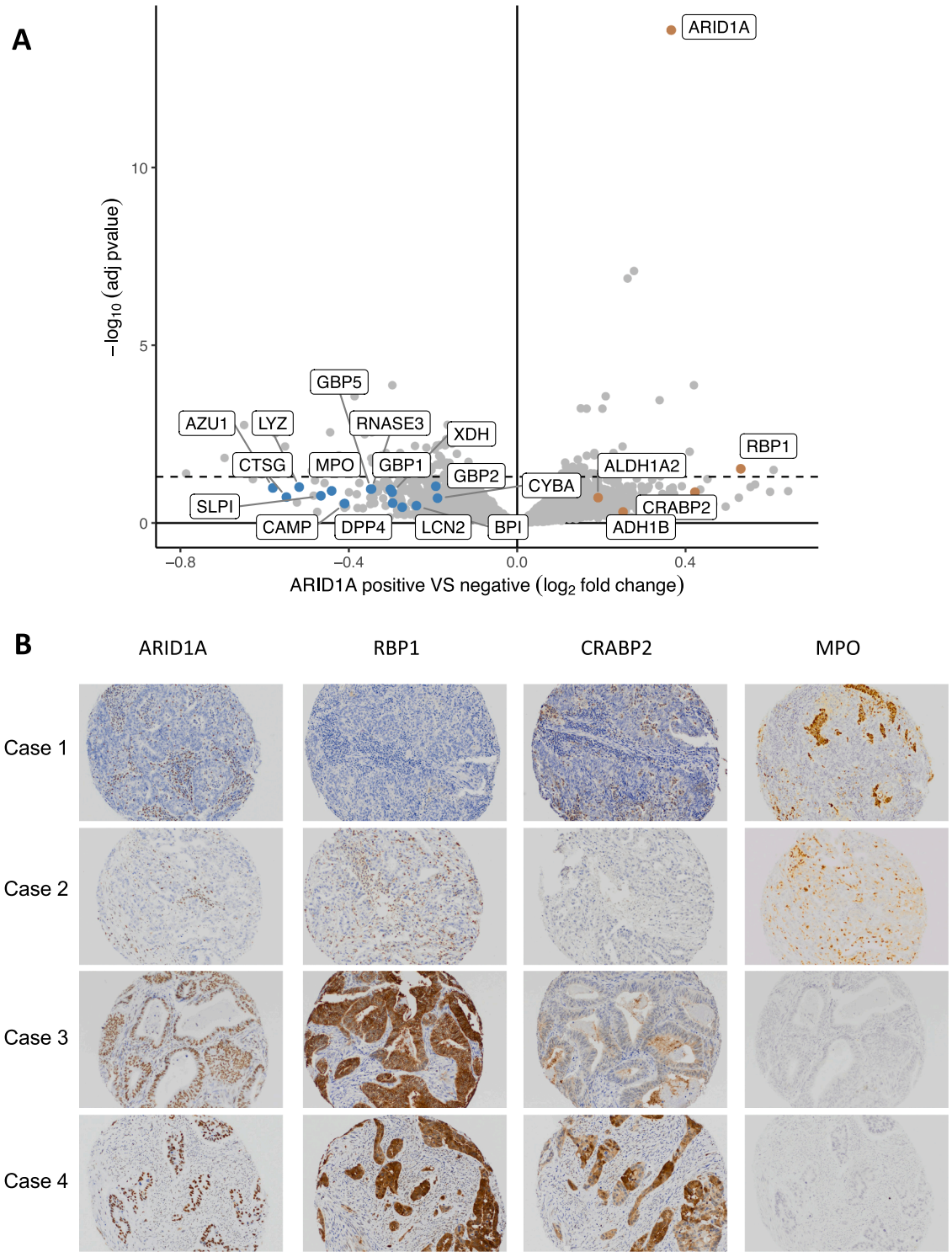

Fig. 4. Correlation between ARID1A expression and retinoic acid pathway and neutrophil infiltration. A. Volcano plot of proteins showing higher abundance in ARID1A positive (right side) or ARID1A negative (left side) tumors with proteins related to the retinoic acid pathway and bacterial response/neutrophils highlighted. **B.** Endometrial tumor TMA (16-005, 475 cases) was immunostained for ARID1A, RBP1, CRABP2 and MPO with representative images shown (20X magnification).

cells with CRISPR-Cas9 depletion of ARID1A, the organoids were larger than organoids expressing ARID1A (Fig. S10C), and RBP1 levels were decreased compared to the normal organoids (Fig. S9D).

Proteins related to outcomes

Survival analysis, demonstrating the association of proteins to disease specific survival (DSS) are shown in Figs. 5 and S10. Among the proteins showing potential prognostic value across the whole cohort of endometrial cancers (all molecular subtypes), TOMM34, TSFM, PXDN, and XPNPEP3 appeared promising. We tested multiple antibodies for validation by IHC, however, the available antibodies did not have the sensitivity and specificity needed for validation studies (PXDN, XPNPEP3) or failed to show a statistically significant difference in

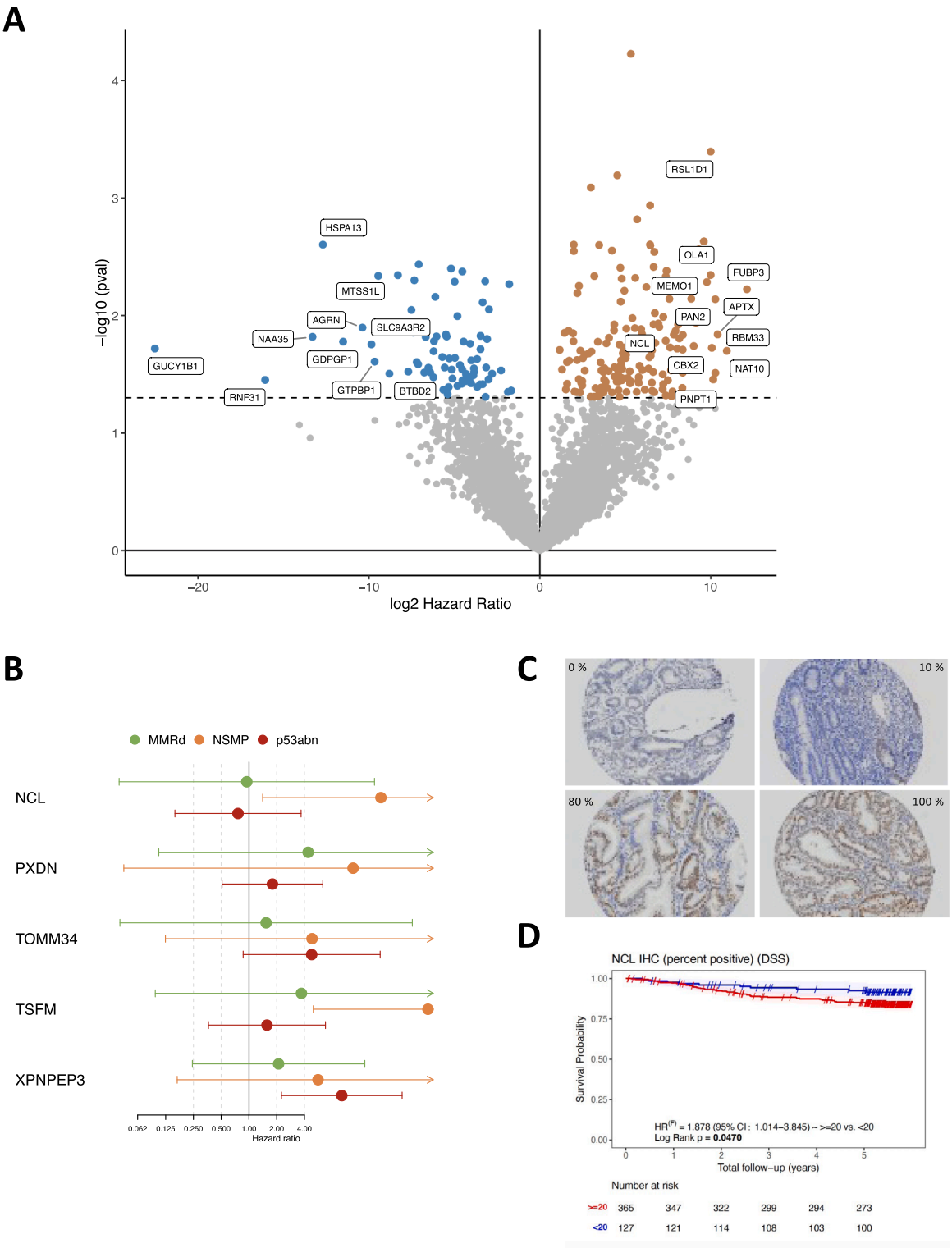

Fig. 5. Proteins associated with clinical outcomes. A. Volcano plot of disease specific survival hazard ratios within the NSMP subtype. **B.** Forest plot showing hazard ratios within MMRd, NSMP, and p53abn subtypes for selected proteins. **C.** Endometrial tumor TMA (16-005, 475 cases) was stained for NCL. Images of different percent positive NCL staining are shown (Magnification 20X). **D.** Kaplan-Meier curve for progression free survival for high and low NCL percent positive.

survival in our validation cohort (TOMM34, TSFM, data not shown). We also looked at specific proteins within the ProMisE molecular subtypes, and found that NCL was associated with worse DSS within the NSMP group (Fig. 5A). In a cohort of 157 endometrial cancers (TMA 11-010), there was worse DSS within the NSMP group using the optimal cut point in percent positive scoring (HR=9.656, p= 0.0331, Fig. S11). In a second larger cohort of 475 endometrial cancers (TMA 16-005), there was no significant difference found in DSS within the NSMP group (not shown), however there was a significant difference in DSS over the whole cohort (HR = 1.878, p= 0.0470, Fig. 5C, D).

Discussion

Molecular classification in endometrial cancer has enabled consistent pathology classification and reporting, informs prognosis and risk group assignment, and can direct adjuvant conventional or targeted therapies. We performed SP3-CTP [22] proteomic characterization of endometrial cancers to potentially further refine molecular classification, analyzing 148 unique endometrial tumors derived from FFPE materials, including 34 *POLE*mut, 40 MMRd, 35 p53abn, and 39 NSMP tumors. We observed a high degree of reproducibility between replicate proteomic samples taken from the same patient and different areas of the hysterectomy specimen. While the reproducibility was still very high, the samples with the most variability were in the patients with *POLE*mut tumors, which carry a very high mutational burden (ultra-mutated) and have high genomic intra-tumoral heterogeneity.

Our study included 23 endometrial biopsies, of which 22 also had matched hysterectomy specimens from the same individual. Hysterectomies are generally performed several weeks to months after endometrial biopsy. We were able to achieve high quality proteomic data from biopsy specimens, and demonstrate a high degree of concordance with the matched biopsy-hysterectomy samples, suggesting the protein expression in these tumors remains relatively stable between the time of biopsy to hysterectomy. The ability to achieve whole proteome profiling from biopsy is extremely important as increasingly, molecular classification of endometrial cancer is being performed on these diagnostic samples and used to direct surgery and treatment, therefore proteomic refinement at this early time point would be hugely beneficial. Notably, we found an enrichment of blood proteins in biopsy samples and extracellular matrix proteins in the hysterectomy samples, both of which would need to be taken into account in interpreting proteomic data in future studies, and with removal of these components the concordance between samples from the same patient was increased.

Unsupervised clustering of the proteomic data from all 4 molecular subtypes of endometrial cancer generated four clusters; 'Adhesion', 'Immune', 'Proliferation', and 'Metabolic'. Pathway analysis showed enrichment for pathways involved DNA replication, transcription, and translation in the 'Proliferation' cluster. The proteins expressed in tumors of the 'Proliferation' cluster are associated with a high rate of proliferation and markers of poor outcome, such as a serous histotype and p53abn subtype. The proteins included ISG15, PRKDC, MCM4, and MCM6 [34,56–58] which are proliferation markers, STAT1, a protein associated with serous endometrial cancer (most of which are p53abn) [59], and LINE-1, which has been correlated with p53abn endometrial tumors, copy number alteration and replication stress [33,60]. The majority of patients in the 'Proliferation' cluster had tumors of p53abn subtype, high stage and grade, non-endometrioid histotype, and more rapid progression events (within two years) than the other clusters. Survival for the 'Proliferation' cluster was worse compared to the other clusters, as would be expected with a higher proportion of p53abn and high stage cases. However, there are patients in molecular subtypes other than p53abn that do unexpectedly poorly and it is possible that the tumors that cluster with the p53abn in the 'Proliferation" have similar underlying biology, such as a high proliferative rate, and are at higher risk of recurrence.

As the leukocyte activation pathway was associated with Cluster 2, as well as proteins expressed by immune cells (LYZ, MPO1, AZU1) it was named the 'Immune' cluster. Interestingly, this cluster was not enriched in MMRd and POLEmut tumors (although representatives from these and all molecular subtypes were noted) and had more p53abn, high stage, and high grade cases compared to the 'Adhesion' and 'Metabolic' clusters. Despite the high proportion of p53abn endometrial cancers the 'Immune' cluster had the better survival of all the clusters. The improved survival may be explained by a high level of immune infiltrates, which has been associated with better outcomes in endometrial cancer and other cancers. There is already strong evidence and FDA approval for ICI therapy in MMRd endometrial tumors, however, there is a great need to identify additional biomarkers to determine which mismatch repair proficient (MMRp) endometrial cancers may benefit from ICI's. The Cluster 2 'Immune' proteomic subset may represent an opportunity to identify patients who may benefit from ICI's [61–66], which would need testing in a prospective cohort.

The 'Metabolic' and 'Adhesion' clusters had intermediate survival and consist largely of endometrioid histotype. While these clusters provide little information on prognosis, they do give insight into the biology underlying the tumors in these two clusters. Proteins enriched in the 'Adhesion' cluster compared to the other clusters include proteins involved in cell-cell adhesion and the actin cytoskeleton (CNN1, TAGLN, TPM1) [67–69] which may serve to enhance tumor cell motility. In the 'Metabolic' cluster, protein expression fell into pathways involved in purine nucleotide metabolism and nucleotide-sugar biosysthesis. Purines are building blocks of RNA and DNA, and provide energy to the cell which is required for proliferation, and purine metabolism is often altered in cancers [70]. Biosynthesis of nucleotide sugars is necessary for glycosylation of cell surface proteins, which in turn can affect cell-cell interactions, communication, and motility [71].

Comparisons of differential protein expression between serous and endometrioid histotypes in our data were consistent with previous studies demonstrating enrichment of UCHL1, HMGA1, and TP53 (p53) in serous tumors [32,72]. Additionally, serous cancers expressed proteins involved in invasion and metastasis (IGF2BP3, UCHL1) [32,73], poor prognosis (IGF2BP3, UCHL1, BCAM, HMGA1) [32,72–74], and interferon response (MX1, STAT1) [59,75]. In contrast, endometrioid histology tumors expressed proteins related to better prognosis (PIGR, ASRGL1) [51,76,77], estrogen receptor positivity (KIAA1324) [78], and metabolism (ASRGL1, HGD) [51].

We compared the present proteomic study to a previous study of 95 tumors, of which 83 were endometrioid and 12 serous [28]. In addition to global proteomics, their cohort was also characterized using phospho-proteomics, genomics and epigenomics. The distribution of molecular subtypes in the Dou et al. proteomic cohort was more similar to the population with 7% POLE ultramutated (*POLE*mut), 26% MSI hypermutated (MMRd), 21% CN-high (p53abn), and 45% CN-low (NSMP), whereas our cohort represented a more balanced distribution. The Dou et al. cohort was collected prospectively and therefore did not have outcome data, while our cohort was retrospective with clinical follow up. The protein expression patterns within molecular subtypes in our cohort and those found by Dou et al. [28] were largely similar, particularly within the NSMP, p53abn, and MMRd subtypes ($p<2.2e-16$). The lowest correlations between our studies and that in Dou et al. were in the *POLE*mut tumors. *POLE*mut tumors have an ultramutator phenotype with greater than 100 mutations per megabase [79] and the intratumoral heterogeneity in *POLE*mut tumors is observed visually in *POLE*mut tumors that also have *TP53* mutations, frequently displaying a subclonal abnormal p53 IHC pattern [80]. Given the ultramutator phenotype and the high degree of intratumoral heterogeneity, it is expected that the least amount of correlation in protein expression between the two studies is observed in the *POLE*mut subtype. Despite the lesser degree of correlation, the expression of some proteins was consistent between the two studies. The *POLE*mut tumors in both our studies and Dou et al. were enriched for Histone H1.1 proteins. An accumulation of histone genes in cancers with *POLE* mutations have previously been described [81], as well as an increase in origins of replication among histone genes [82]. Since origins of replication tend to be around transcriptional start sites and in areas of open chromatin, the accumulation of replication origins near histone genes may be indicative of more transcriptional activity in these areas, leading to an increased abundance of histone proteins.

RPL22L1 was found to be enriched in our patients of MMRd subtype, as has been previously reported [28]. Increased expression of RPL22L1 protein could be a way to compensate for frequent mutations of its homolog, RPL22, in tumors with microsatellite instability [83]. RPL22L1 has been found to promote proliferation, migration, invasion, and

therapy resistance in several cancer types [84–86] and could perform similar functions in MMRd endometrial cancers. In addition, proteins involved in various steroid hormone signaling pathways were abundant in MMRd tumors compared to other subtypes including NSMP tumors where we had predicted enrichment. These proteins included PDIA2, which in benign endometrial tissue has lower expression levels in secretory as compared to proliferative endometrium [43], and SCGB2A1 and SCGB1D2, which are transcriptional targets of the androgen receptor [44]. Proteins involved in polarity and cell adhesion, such as PATK, CEACAM5, and LAD1 were found to be highly expressed in MMRd tumors. These proteins have been linked to increased migration, invasion and anoikis resistance [87–94].

Some of the proteins expressed highly in NSMP tumors are often expressed in normal cells and are associated with tumors and better outcomes. The keratins found to be expressed more highly in NSMP tumors compared to other subtypes (KRT5, KRT6A, and KRT75) are basal cell markers and can be also found in endometrial hyperplasia [95]. In the uterus, EZH2 represses abnormal stratification of the epithelium and expression of KRT5 and KRT6A [95–97]. Similarly, the estrogen receptor (ER) also controls expression of basal cell keratins (KRT5, KRT6) in normal endometrium and excess ER signaling has been linked to endometrial hyperplasia [98,99]. EZH2 and the ER work together during uterine development to ensure proper epithelial differentiation [100]. Loss of EZH2 and excess ER signaling are indicative of endometrial cancer precursors and early tumorigenesis, aberrant high EZH2 expression and loss of ER are features of more aggressive endometrial tumors [101–103]. As NSMP tumors express keratins that suggests they retain EZH2 and ER signaling, this is consistent with NSMP tumors often being low grade and having good outcomes. Compared to the other three molecular subytpes, our NSMP tumors also expressed higher levels of ASRGL1, a metabolic protein that is usually lost in more aggressive endometrial cancers [77,104].

Within p53abn endometrial cancers, p53 protein was more highly expressed compared to the other 3 molecular groups, consistent with most p53abn tumors having missense mutations that cause an accumulation in p53 protein [105,106]. As would be expected, the proteins more highly expressed in the p53abn cases have previously been associated with serous histomorphology and more aggressive features. We also found GRB7 to be expressed at high levels in p53abn tumors. GRB7 is an adaptor protein that interacts with receptor tyrosine kinases, including EGFR and HER2 [107]. The *GRB7* gene is near the *ERBB2* (HER2) gene, and in several cancer types including breast [38,108], esophageal [40,42], and gastric cancers [109], *ERBB2* and *GRB7* are co-amplified and both overexpressed. Co-overexpression of GRB7 and HER2 leads to worse clinical outcomes compared to overexpression of HER2 alone [110]. Overexpression of GRB7 decreases apoptosis and increases proliferation, migration, invasion, and metastasis [111–116]. In our data, there was poor correlation between GRB7 and HER2 protein expression, suggesting that in our cohort, overexpression of GRB7 was not necessarily linked to *GRB7* and *ERBB2* co-amplification in most cases. In our cohort we found that high GRB7 expression was associated with poor survival. Pre-clinical studies on peptides that bind the SH2 domain of GRB7, preventing interaction with receptor tyrosine kinases have showed promise in blocking migration, invasion, and metastasis in experimental model systems [117–119]. This suggests that GRB7 may be a targetable feature for patients with p53abn endometrial cancers.

Some recurrent mutations appear across all molecular subtypes, including *ARID1A* mutations resulting in loss of ARID1A protein expression; observed in up to 60% of endometrial cancers [53–55]. We performed differential protein abundance analysis on endometrial tumors that expressed ARID1A and those that do not express ARID1A. We used IHC to determine ARID1A expression and while we did not have mutation data, most ARID1A deficient tumors will be the result of *ARID1A* mutations [55]. We found that tumors with loss of ARID1A expression were enriched with proteins related to an anti-microbial/neutrophil response. There are many cancer types in which tumor associated neutrophils (TANs) have been associated with poor prognosis [120–124], however this is complicated by some reports of TANs being associated with good prognosis [125,126]. This may suggest that there is a context specific effect of TANs that remains to be elucidated. In a mouse model of endometrial cancer, neutrophils inhibit tumor formation and progression [127]. There have been some links with Arid1A loss and immune response in mouse models. In *Arid1A* knockout mice, the inflammatory response is decreased with fewer neutrophils being recruited in the skin in response to damage [128]. Arid1A loss in the liver resulted in higher levels of neutrophil infiltration compared to Arid1A proficient livers, and the hepatocellular carcinomas arising in the *Arid1A* knockout mice displayed higher neutrophil infiltration compared to adjacent normal tissue [129]. TANs may play a significant role in resistance to immunotherapy and anti-angiogenesis therapies [130,131], and therefore this could be a consideration when designing targeted treatments for ARID1A deficient endometrial tumors.

In tumors with ARID1A expression, we observed increased expression of proteins involved in retinoic acid signaling, including RBP1, which binds retinol in the cytoplasm and CRABP2, which transports retinoic acid to the nucleus where it interacts with retinoic acid receptors to affect transcription. We demonstrate that depletion of ARID1A in cell lines and organoid molecules causes a decrease in RBP1 protein levels. Retinoic acid signaling is important for differentiation in the endometrium. RBP1 is expressed in normal endometrial epithelium and tends to be lost in atypical endometrial hyperplasia and in some endometrial tumors, with levels decreasing with higher tumor grade [132,133]. High CRABP2 expression is associated with poor survival in endometrial cancer [134,135]. The role of retinoic acid signaling as it relates to ARID1A remains to be elucidated.

The proteomic data were analyzed across the full endometrial cancer cohort and within the four molecular subtypes to test for associations with individual proteins and clinical outcomes. While some statistically significant differences in survival based of the expression of some proteins were found, the outcomes were not large enough or consistent enough to be of immediate clinical utility, but could be useful in understanding how the expression of some proteins impact the biology of the tumors and resultant clinical outcome variability. We found high nucleolin (NCL) to be associated with poor survival in NSMP subtype patients and confirmed this using IHC assessment in a small cohort of 157 endometrial cancers. In a second larger validation cohort of 475 endometrial cancers, NCL expression was associated with worse prognosis overall but not within NSMP. NCL has been previously reported to be prognostic in endometrial cancer [136,137], however molecular subtypes were not taken into consideration in these other series. In future studies, it would be informative to test the value of NCL in refining prognosis within NSMP tumors in the context of other known stratification features, such as artificial intelligence histopathology image analysis [138], and/or ER expression levels [139,140]. While the primary function of NCL in the cell is in rRNA and ribosome biosynthesis, NCL has been implicated in many cellular functions including cell cycle, apoptosis, DNA replication and repair, telomerase regulation, and chromatin remodeling [141].While the majority of NCL expression is in the nucleus, NCL can be expressed to some degree in the cytoplasm and plasma membrane of tumor cells [142,143]. Since NCL is expressed on the cell surface of tumor cells at a much higher level than normal cells, efforts are being made to use it to direct therapeutics, either to bind ligands that will deliver a toxic agent or as a target of immunotherapy [144–148]. It remains to be seen whether NCL is expressed at high enough levels in the cytoplasm to make it a viable therapeutic target in endometrial cancers.

While other studies have included proteomic analyses that include protein modifications, such as phospho-, acetyl-, and glyco-proteomics on prospective cohorts [28,149], we focused on global proteomic characterization of a retrospective cohort of molecularly defined endometrial cancers that have been well characterized, with associated clinical and outcome data, and cohorts of characterized endometrial

cancers used for validation. We were able to achieve a large proteomic dataset from FFPE materials. With 148 individual endometrial tumors, we were able to define proteomic clusters that were largely independent of molecular subtype, with the exception of an enrichment of p53abn cases in the proliferative cluster. These proteomic clusters contribute towards a better understanding of the biology underpinning this disease and the diversity that exists within the molecular subtypes. We found differences in protein expression between tumors grouped by pathologist assigned histotypes, ARID1A protein expression, and outcomes. However, the relatively small number of cases within each of the molecular subtypes, and the diversity of profiles within subtypes (especially within the highly mutated *POLE*mut tumors) limits further conclusions from our data.

We anticipate additional molecular, proteomic and biomarker studies linked to outcomes may add further stratification to endometrial cancer molecular classification. Our study thus provides both the experimental replication and justification for future functional and biomarker studies to better define and clarify diagnostic and prognostic biomarkers, and for the investigation of driving oncogenic processes for potential treatments.

CRediT authorship contribution statement

Dawn R. Cochrane: Writing – review & editing, Writing – original draft, Visualization, Validation, Supervision, Conceptualization. **Gian Luca Negri:** Writing – review & editing, Visualization, Software, Investigation, Formal analysis, Conceptualization. **Jutta Huvila:** Investigation. **Forouh Kalantari:** Visualization, Investigation. **David A. Farnell:** Investigation. **Nissreen Mohammad:** Investigation. **Emily Thompson:** Investigation. **Winnie Yang:** Investigation. **Amy Lum:** Investigation. **Sandra E. Spencer:** Methodology, Investigation. **Ryan Riley:** Investigation. **Amy Jamieson:** Investigation, Funding acquisition. **Samuel Leung:** Investigation, Formal analysis, Data curation. **Derek Chiu:** Investigation, Formal analysis. **Christine Chow:** Investigation. **Jamie L.P. Lim:** Investigation. **Martin Köbel:** Investigation. **Stefan Kommoss:** Methodology. **Friedrich Kommoss:** Methodology. **Blake Gilks:** Investigation. **Lien Hoang:** Project administration, Investigation. **David G. Huntsman:** Supervision, Funding acquisition, Conceptualization. **Gregg B. Morin:** Writing – review & editing, Supervision, Project administration, Conceptualization. **Jessica N. McAlpine:** Writing – review & editing, Project administration, Funding acquisition, Conceptualization.

Declaration of competing interest

The authors declare that they have no known competing financial interests or personal relationships that could have appeared to influence the work reported in this paper.

Acknowledgements

This work was supported by a Canadian Cancer Society Research Institute Innovation Grant (# 704388). This team has also been supported by the BC Cancer Foundation (Clinician Scientist Award (JMc)), the Chew Wei Chair in Gynecologic Oncology (JMc), the Chew Wei Professorship in Gynecologic Oncology (DGH) and the Canada Research Chairs program (Research Chair in Molecular and Genomic Pathology (DGH), and Molecular stratification of Gynecologic Cancers (JMc)) and the Miller-Mindell Fellowship (AJ). We wish to acknowledge support from the BC Cancer Foundation and the VGH and UBC Hospital Foundation to OVCARE.

Supplementary materials

Supplementary material associated with this article can be found, in the online version, at doi:10.1016/j.neo.2025.101229.

References

[1] D.A. Levine, The Cancer Genome Atlas Research Network, Integrated genomic characterization of endometrial carcinoma, Nature 497 (2013) 67–73, https://doi.org/10.1038/nature12113.
[2] N. Abu-Rustum, et al., Uterine neoplasms, version 1.2023, NCCN clinical practice guidelines in oncology, J. Natl. Compr. Cancer Netw. 21 (2023) 181–209, https://doi.org/10.6004/jnccn.2023.0006.
[3] J.S. Berek, et al., FIGO staging of endometrial cancer: 2023, J. Gynecol. Oncol. 34 (2023) e85, https://doi.org/10.3802/jgo.2023.34.e85.
[4] N. Concin, et al., ESGO/ESTRO/ESP guidelines for the management of patients with endometrial carcinoma, Int. J. Gynecol. Cancer 31 (2021) 12–39, https://doi.org/10.1136/ijgc-2020-002230.
[5] S. Kommoss, et al., Final validation of the ProMisE molecular classifier for endometrial carcinoma in a large population-based case series, Ann. Oncol. 29 (2018) 1180–1188, https://doi.org/10.1093/annonc/mdy058.
[6] A. Talhouk, et al., A clinically applicable molecular-based classification for endometrial cancers, Br. J. Cancer 113 (2015) 299–310, https://doi.org/10.1038/bjc.2015.190.
[7] A. Talhouk, et al., Confirmation of ProMisE: a simple, genomics-based clinical classifier for endometrial cancer, Cancer 123 (2017) 802–813, https://doi.org/10.1002/cncr.30496.
[8] E. Stelloo, et al., Refining prognosis and identifying targetable pathways for high-risk endometrial cancer; a TransPORTEC initiative, Mod. Pathol. 28 (2015) 836–844, https://doi.org/10.1038/modpathol.2015.43.
[9] J. McAlpine, A. Leon-Castillo, T. Bosse, The rise of a novel classification system for endometrial carcinoma; integration of molecular subclasses, J. Pathol. 244 (2018) 538–549, https://doi.org/10.1002/path.5034.
[10] A. Jamieson, J.N. McAlpine, Molecular profiling of endometrial cancer from TCGA to clinical practice, J. Natl. Compr. Cancer Netw. 21 (2023) 210–216, https://doi.org/10.6004/jnccn.2022.7096.
[11] R.R. Consortium, Refining adjuvant treatment in endometrial cancer based on molecular features: the RAINBO clinical trial program, Int. J. Gynecol. Cancer 33 (2022) 109–117, https://doi.org/10.1136/ijgc-2022-004039.
[12] R.N. Eskander, et al., Pembrolizumab plus chemotherapy in advanced endometrial cancer, N. Engl. J. Med. 388 (2023) 2159–2170, https://doi.org/10.1056/NEJMoa2302312.
[13] M.R. Mirza, et al., Dostarlimab for primary advanced or recurrent endometrial cancer, N. Engl. J. Med. 388 (2023) 2145–2158, https://doi.org/10.1056/NEJMoa2216334.
[14] Y. Gao, et al., Quantitative proteomics by SWATH-MS reveals sophisticated metabolic reprogramming in hepatocellular carcinoma tissues, Sci. Rep. 7 (2017) 45913, https://doi.org/10.1038/srep45913.
[15] Y. Zhu, et al., Identification of protein abundance changes in hepatocellular carcinoma tissues using PCT-SWATH, Proteom. Clin. Appl. 13 (2019) e1700179, https://doi.org/10.1002/prca.201700179.
[16] J.X. Ji, et al., The proteome of clear cell ovarian carcinoma, J. Pathol. 258 (2022) 325–338, https://doi.org/10.1002/path.6006.
[17] A.F. Busso-Lopes, et al., Connecting multiple microenvironment proteomes uncovers the biology in head and neck cancer, Nat. Commun. 13 (2022) 6725, https://doi.org/10.1038/s41467-022-34407-1.
[18] P. Bouchal, et al., Breast cancer classification based on proteotypes obtained by SWATH mass spectrometry, Cell Rep. 28 (2019) 832–843, https://doi.org/10.1016/j.celrep.2019.06.046, e837.
[19] K. Asleh, et al., Proteomic analysis of archival breast cancer clinical specimens identifies biological subtypes with distinct survival outcomes, Nat. Commun. 13 (2022) 896, https://doi.org/10.1038/s41467-022-28524-0.
[20] A.S. Ho, et al., Comparative proteomic analysis of HPV(+) oropharyngeal squamous cell carcinoma recurrence, J. Proteome Res. 21 (2022) 200–208, https://doi.org/10.1021/acs.jproteome.1c00757.
[21] S. Satpathy, et al., Microscaled proteogenomic methods for precision oncology, Nat. Commun. 11 (2020) 532, https://doi.org/10.1038/s41467-020-14381-2.
[22] C.S. Hughes, et al., Single-pot, solid-phase-enhanced sample preparation for proteomics experiments, Nat. Protoc. 14 (2019) 68–85, https://doi.org/10.1038/s41596-018-0082-x.
[23] Y. Zhu, et al., DEqMS: a method for accurate variance estimation in differential protein expression analysis, Mol. Cell. Proteom. 19 (2020) 1047–1057, https://doi.org/10.1074/mcp.TIR119.001646.
[24] Korotkevich, G. et al. Fast gene set enrichment analysis. bioRxiv, 060012, doi:10.1101/060012 (2021).
[25] A. Subramanian, et al., Gene set enrichment analysis: a knowledge-based approach for interpreting genome-wide expression profiles, Proc. Natl. Acad. Sci. USA 102 (2005) 15545–15550, https://doi.org/10.1073/pnas.0506580102.
[26] S. Monti, P. Tamayo, J. Mesirov, T. Golub, Consensus clustering: a resampling-based method for class discovery and visualization of gene expression microarray data, Mach. Learn. 52 (2003) 91–118, https://doi.org/10.1023/A:1023949509487.
[27] M.D. Wilkerson, D.N. Hayes, ConsensusClusterPlus: a class discovery tool with confidence assessments and item tracking, Bioinformatics 26 (2010) 1572–1573, https://doi.org/10.1093/bioinformatics/btq170.
[28] Y. Dou, et al., Proteogenomic characterization of endometrial carcinoma, Cell 180 (2020) 729–748, https://doi.org/10.1016/j.cell.2020.01.026, e726.
[29] https://proteomic.datacommons.cancer.gov/pdc/.
[30] Y. Perez-Riverol, et al., The PRIDE database resources in 2022: a hub for mass spectrometry-based proteomics evidences, Nucleic Acids Res. 50 (2022) D543–D552, https://doi.org/10.1093/nar/gkab1038.

[31] K. Nakao, et al., High expression of ubiquitin C-terminal hydrolase L1 is associated with poor prognosis in endometrial cancer patients, Int. J. Gynecol. Cancer 28 (2018) 675–683, https://doi.org/10.1097/IGC.0000000000001201.

[32] S.Y. Kwan, et al., Ubiquitin carboxyl-terminal hydrolase L1 (UCHL1) promotes uterine serous cancer cell proliferation and cell cycle progression, Cancers 12 (2020), https://doi.org/10.3390/cancers12010118.

[33] W. McKerrow, et al., LINE-1 expression in cancer correlates with p53 mutation, copy number alteration, and S phase checkpoint, Proc. Natl. Acad. Sci. USA 119 (2022), https://doi.org/10.1073/pnas.2115999119.

[34] X. Zhao, et al., Interferon-stimulated gene 15 promotes progression of endometrial carcinoma and weakens antitumor immune response, Oncol. Rep. 47 (2022), https://doi.org/10.3892/or.2022.8321.

[35] W. Zheng, et al., The oncofetal protein IMP3: a novel biomarker for endometrial serous carcinoma, Am. J. Surg. Pathol. 32 (2008) 304–315, https://doi.org/10.1097/PAS.0b013e3181483ff8.

[36] P. Mhawech-Fauceglia, et al., IMP3 distinguishes uterine serous carcinoma from endometrial endometrioid adenocarcinoma, Am. J. Clin. Pathol. 133 (2010) 899–908, https://doi.org/10.1309/AJCPQDQXJ4FNRFQB.

[37] C. Li, et al., Expression of a novel oncofetal mRNA-binding protein IMP3 in endometrial carcinomas: diagnostic significance and clinicopathologic correlations, Mod. Pathol. 20 (2007) 1263–1268, https://doi.org/10.1038/modpathol.3800960.

[38] K.K. Sahlberg, et al., The HER2 amplicon includes several genes required for the growth and survival of HER2 positive breast cancer cells, Mol. Oncol. 7 (2013) 392–401, https://doi.org/10.1016/j.molonc.2012.10.012.

[39] M. Saito, et al., Expression screening of 17q12-21 amplicon reveals GRB7 as an ERBB2-dependent oncogene, FEBS Lett. 586 (2012) 1708–1714, https://doi.org/10.1016/j.febslet.2012.05.003.

[40] P.S. Dahlberg, et al., ERBB2 amplifications in esophageal adenocarcinoma, Ann. Thorac. Surg. 78 (2004) 1790–1800, https://doi.org/10.1016/j.athoracsur.2004.05.037.

[41] A. Walch, et al., Coamplification and coexpression of GRB7 and ERBB2 is found in high grade intraepithelial neoplasia and in invasive Barrett's carcinoma, Int. J. Cancer 112 (2004) 747–753, https://doi.org/10.1002/ijc.20411.

[42] S. Tanaka, et al., Coexpression of Grb7 with epidermal growth factor receptor or Her2/erbB2 in human advanced esophageal carcinoma, Cancer Res. 57 (1997) 28–31.

[43] S.R. Fernando, et al., Differential expression of protein disulfide isomerase (PDI) in regulating endometrial receptivity in humans, Reprod. Biol. 21 (2021) 100498, https://doi.org/10.1016/j.repbio.2021.100498.

[44] F. Xiao, A. Mirwald, M. Papaioannou, A. Baniahmad, J. Klug, Secretoglobin 2A1 is under selective androgen control mediated by a peculiar binding site for Sp family transcription factors, Mol. Endocrinol. 19 (2005) 2964–2978, https://doi.org/10.1210/me.2004-0408.

[45] M. Zafrakas, et al., Expression analysis of mammaglobin A (SCGB2A2) and lipophilin B (SCGB1D2) in more than 300 human tumors and matching normal tissues reveals their co-expression in gynecologic malignancies, BMC Cancer 6 (2006) 88, https://doi.org/10.1186/1471-2407-6-88.

[46] R.D. Blumenthal, H.J. Hansen, D.M. Goldenberg, Inhibition of adhesion, invasion, and metastasis by antibodies targeting CEACAM6 (NCA-90) and CEACAM5 (Carcinoembryonic antigen), Cancer Res. 65 (2005) 8809–8817, https://doi.org/10.1158/0008-5472.CAN-05-0420.

[47] N.A. Mack, M. Georgiou, The interdependence of the Rho GTPases and apicobasal cell polarity, Small GTPases 5 (2014) 10, https://doi.org/10.4161/21541248.2014.973768.

[48] M. Klobucar, et al., Basement membrane protein ladinin-1 and the MIF-CD44-beta1 integrin signaling axis are implicated in laryngeal cancer metastasis, Biochim. Biophys. Acta 1862 (2016) 1938–1954, https://doi.org/10.1016/j.bbadis.2016.07.014.

[49] C. Zeng, et al., DPEP1 promotes drug resistance in colon cancer cells by forming a positive feedback loop with ASCL2, Cancer Med. 12 (2023) 412–424, https://doi.org/10.1002/cam4.4926.

[50] J. Quan, A.M. Bode, X. Luo, ACSL family: the regulatory mechanisms and therapeutic implications in cancer, Eur. J. Pharmacol. 909 (2021) 174397, https://doi.org/10.1016/j.ejphar.2021.174397.

[51] J. Huvila, et al., Combined ASRGL1 and p53 immunohistochemistry as an independent predictor of survival in endometrioid endometrial carcinoma, Gynecol. Oncol. 149 (2018) 173–180, https://doi.org/10.1016/j.ygyno.2018.02.016.

[52] A. Saha, Y. Dalal, A glitch in the snitch: the role of linker histone H1 in shaping the epigenome in normal and diseased cells, Open Biol. 11 (2021) 210124, https://doi.org/10.1098/rsob.210124.

[53] M.K. McConechy, et al., Use of mutation profiles to refine the classification of endometrial carcinomas, J. Pathol. 228 (2012) 20–30, https://doi.org/10.1002/path.4056.

[54] Y. Wang, L. Hoang, J.X. Ji, D.G. Huntsman, SWI/SNF complex mutations in gynecologic cancers: molecular mechanisms and models, Annu. Rev. Pathol. 15 (2020) 467–492, https://doi.org/10.1146/annurev-pathmechdis-012418-012917.

[55] K.C. Wiegand, et al., Loss of BAF250a (ARID1A) is frequent in high-grade endometrial carcinomas, J. Pathol. 224 (2011) 328–333, https://doi.org/10.1002/path.2911.

[56] Y. Liu, et al., Protein kinase D3 promotes the cell proliferation by activating the ERK1/c-MYC axis in breast cancer, J. Cell. Mol. Med. 24 (2020) 2135–2144, https://doi.org/10.1111/jcmm.14772.

[57] Y. Xu, et al., MCM4 in human hepatocellular carcinoma: a potent prognostic factor associated with cell proliferation, Biosci. Trends 15 (2021) 100–106, https://doi.org/10.5582/bst.2021.01016.

[58] Y. Luo, et al., UBE3A and MCM6 synergistically regulate the proliferation and migration of lung adenocarcinoma cells, FEBS Open Bio 13 (2023) 1756–1771, https://doi.org/10.1002/2211-5463.13675.

[59] B. Kharma, et al., STAT1 drives tumor progression in serous papillary endometrial cancer, Cancer Res. 74 (2014) 6519–6530, https://doi.org/10.1158/0008-5472.CAN-14-0847.

[60] Z. Xia, et al., Expression of L1 retrotransposon open reading frame protein 1 in gynecologic cancers, Hum. Pathol. 92 (2019) 39–47, https://doi.org/10.1016/j.humpath.2019.06.001.

[61] R.A. de Jong, et al., Presence of tumor-infiltrating lymphocytes is an independent prognostic factor in type I and II endometrial cancer, Gynecol. Oncol. 114 (2009) 105–110, https://doi.org/10.1016/j.ygyno.2009.03.022.

[62] S. Kondratiev, E. Sabo, E. Yakirevich, O. Lavie, M.B. Resnick, Intratumoral CD8+ T lymphocytes as a prognostic factor of survival in endometrial carcinoma, Clin. Cancer Res. 10 (2004) 4450–4456, https://doi.org/10.1158/1078-0432.CCR-0732-3.

[63] H.H. Workel, et al., CD103 defines intraepithelial CD8+ PD1+ tumour-infiltrating lymphocytes of prognostic significance in endometrial adenocarcinoma, Eur. J. Cancer 60 (2016) 1–11, https://doi.org/10.1016/j.ejca.2016.02.026.

[64] A. Lopez-Janeiro, et al., The association between the tumor immune microenvironments and clinical outcome in low-grade, early-stage endometrial cancer patients, J. Pathol. 258 (2022) 426–436, https://doi.org/10.1002/path.6012.

[65] B. Wu, B. Zhang, B. Li, H. Wu, M. Jiang, Cold and hot tumors: from molecular mechanisms to targeted therapy, Signal Transduct. Target. Ther. 9 (2024) 274, https://doi.org/10.1038/s41392-024-01979-x.

[66] L. Wang, et al., Hot and cold tumors: immunological features and the therapeutic strategies, MedComm. (2020) 4 (2023) e343, https://doi.org/10.1002/mco2.343.

[67] W. Liu, X. Fu, R. Li, CNN1 regulates the DKK1/Wnt/beta-catenin/c-myc signaling pathway by activating TIMP2 to inhibit the invasion, migration and EMT of lung squamous cell carcinoma cells, Exp. Ther. Med. 22 (2021) 855, https://doi.org/10.3892/etm.2021.10287.

[68] M. Elsafadi, et al., Transgelin is a TGFbeta-inducible gene that regulates osteoblastic and adipogenic differentiation of human skeletal stem cells through actin cytoskeleston organization, Cell Death Dis. 7 (2016) e2321, https://doi.org/10.1038/cddis.2016.196.

[69] T. Xu, et al., Tropomyosin1 isoforms underlie epithelial to mesenchymal plasticity, metastatic dissemination, and resistance to chemotherapy in high-grade serous ovarian cancer, Cell Death Differ. 31 (2024) 360–377, https://doi.org/10.1038/s41418-024-01267-9.

[70] J. Yin, et al., Potential mechanisms connecting purine metabolism and cancer therapy, Front. Immunol. 9 (2018) 1697, https://doi.org/10.3389/fimmu.2018.01697.

[71] I. Hauselmann, L. Borsig, Altered tumor-cell glycosylation promotes metastasis, Front. Oncol. 4 (2014) 28, https://doi.org/10.3389/fonc.2014.00028.

[72] J. Hillion, et al., The high mobility group A1 (HMGA1) gene is highly overexpressed in human uterine serous carcinomas and carcinosarcomas and drives Matrix Metalloproteinase-2 (MMP-2) in a subset of tumors, Gynecol. Oncol. 141 (2016) 580–587, https://doi.org/10.1016/j.ygyno.2016.03.020.

[73] C. Wang, et al., IGF2BP3 enhances the mRNA stability of E2F3 by interacting with LINC00958 to promote endometrial carcinoma progression, Cell Death Discov. 8 (2022) 279, https://doi.org/10.1038/s41420-022-01045-x.

[74] X. He, et al., Deregulation of cell adhesion molecules is associated with progression and poor outcomes in endometrial cancer: analysis of the cancer genome atlas data, Oncol. Lett. 19 (2020) 1906–1914, https://doi.org/10.3892/ol.2020.11295.

[75] F.H. Tang, W.A. Chang, E.M. Tsai, M.J. Tsai, P.L. Kuo, Investigating novel genes potentially involved in endometrial adenocarcinoma using next-generation sequencing and bioinformatic approaches, Int. J. Med. Sci. 16 (2019) 1338–1348, https://doi.org/10.7150/ijms.38219.

[76] G. Mandal, et al., IgA-dominated humoral immune responses govern patients' outcome in endometrial cancer, Cancer Res. 82 (2022) 859–871, https://doi.org/10.1158/0008-5472.CAN-21-2376.

[77] P.H. Edqvist, et al., Loss of ASRGL1 expression is an independent biomarker for disease-specific survival in endometrioid endometrial carcinoma, Gynecol. Oncol. 137 (2015) 529–537, https://doi.org/10.1016/j.ygyno.2015.03.055.

[78] L. Deng, J. Feng, R.R. Broaddus, The novel estrogen-induced gene EIG121 regulates autophagy and promotes cell survival under stress, Cell Death Dis. 1 (2010) e32, https://doi.org/10.1038/cddis.2010.9.

[79] D.A. Levine, et al., Integrated genomic characterization of endometrial carcinoma, Nature 497 (2013) 67–73, https://doi.org/10.1038/nature12113.

[80] L. Vermij, V. Smit, R. Nout, T. Bosse, Incorporation of molecular characteristics into endometrial cancer management, Histopathology 76 (2020) 52–63, https://doi.org/10.1111/his.14015.

[81] D. Ostroverkhova, D. Espiritu, M.J. Aristizabal, A.R. Panchenko, Leveraging gene redundancy to find new histone drivers in cancer, Cancers 15 (2023), https://doi.org/10.3390/cancers15133437.

[82] R. Jaksik, D.A. Wheeler, M. Kimmel, Detection and characterization of constitutive replication origins defined by DNA polymerase epsilon, BMC Biol. 21 (2023) 41, https://doi.org/10.1186/s12915-023-01527-z.

[83] A.P. Novetsky, et al., Frequent mutations in the RPL22 gene and its clinical and functional implications, Gynecol. Oncol. 128 (2013) 470–474, https://doi.org/10.1016/j.ygyno.2012.10.026.

[84] S. Rao, et al., RPL22L1 induction in colorectal cancer is associated with poor prognosis and 5-FU resistance, PLoS ONE 14 (2019) e0222392, https://doi.org/10.1371/journal.pone.0222392.

[85] Y. Chen, et al., RPL22L1, a novel candidate oncogene promotes temozolomide resistance by activating STAT3 in glioblastoma, Cell Death Dis. 14 (2023) 757, https://doi.org/10.1038/s41419-023-06156-6.

[86] D. Zhang, et al., Ribosomal protein L22-like1 (RPL22L1) mediates sorafenib sensitivity via ERK in hepatocellular carcinoma, Cell Death Discov. 8 (2022) 365, https://doi.org/10.1038/s41420-022-01153-8.

[87] D. Wu, et al., MUC1 and polarity markers INADL and SCRIB identify salivary ductal cells, J. Dent. Res. 101 (2022) 983–991, https://doi.org/10.1177/00220345221076122.

[88] A. Barbachano, et al., SPROUTY-2 represses the epithelial phenotype of colon carcinoma cells via upregulation of ZEB1 mediated by ETS1 and miR-200/miR-150, Oncogene 35 (2016) 2991–3003, https://doi.org/10.1038/onc.2015.366.

[89] X. Zhang, X. Han, P. Zuo, X. Zhang, H. Xu, CEACAM5 stimulates the progression of non-small-cell lung cancer by promoting cell proliferation and migration, J. Int. Med. Res. 48 (2020), https://doi.org/10.1177/0300060520959478, 300060520959478.

[90] H. Yang, et al., Extracellular ATP promotes breast cancer invasion and chemoresistance via SOX9 signaling, Oncogene 39 (2020) 5795–5810, https://doi.org/10.1038/s41388-020-01402-z.

[91] E.Y. Kim, Y.J. Cha, S. Jeong, Y.S. Chang, Overexpression of CEACAM6 activates Src-FAK signaling and inhibits anoikis, through homophilic interactions in lung adenocarcinomas, Transl. Oncol. 20 (2022) 101402, https://doi.org/10.1016/j.tranon.2022.101402.

[92] Y. Jiang, et al., LAD1 promotes malignant progression by diminishing ubiquitin-dependent degradation of vimentin in gastric cancer, J. Transl. Med. 21 (2023) 632, https://doi.org/10.1186/s12967-023-04401-2.

[93] C.Y. Chang, et al., Ladinin 1 shortens survival via promoting proliferation and enhancing invasiveness in lung adenocarcinoma, Int. J. Mol. Sci. (2022) 24, https://doi.org/10.3390/ijms24010431.

[94] K. Shin, Q. Wang, B. Margolis, PATJ regulates directional migration of mammalian epithelial cells, EMBO Rep. 8 (2007) 158–164, https://doi.org/10.1038/sj.embor.7400890.

[95] X. Fang, et al., Enhancer of Zeste 2 polycomb repressive complex 2 subunit is required for uterine epithelial integrity, Am. J. Pathol. 189 (2019) 1212–1225, https://doi.org/10.1016/j.ajpath.2019.02.016.

[96] A.M. Mesa, et al., Mice lacking uterine enhancer of zeste homolog 2 have transcriptomic changes associated with uterine epithelial proliferation, Physiol. Genom. 52 (2020) 81–95, https://doi.org/10.1152/physiolgenomics.00098.2019.

[97] A.M. Mesa, et al., Spatial transcriptomics analysis of uterine gene expression in enhancer of zeste homolog 2 conditional knockout micedagger, Biol. Reprod. 105 (2021) 1126–1139, https://doi.org/10.1093/biolre/ioab147.

[98] J.A. Rizo, K.M. Davenport, W. Winuthayanon, T.E. Spencer, A.M. Kelleher, Estrogen receptor alpha regulates uterine epithelial lineage specification and homeostasis, iScience 26 (2023) 107568, https://doi.org/10.1016/j.isci.2023.107568.

[99] T.M. Kuhn, S. Dhanani, S. Ahmad, An overview of endometrial cancer with novel therapeutic strategies, Curr. Oncol. 30 (2023) 7904–7919, https://doi.org/10.3390/curroncol30090574.

[100] M.K. Nanjappa, et al., The histone methyltransferase EZH2 is required for normal uterine development and function in micedagger, Biol. Reprod. 101 (2019) 306–317, https://doi.org/10.1093/biolre/ioz097.

[101] J.W. Roh, et al., Clinical and biological significance of EZH2 expression in endometrial cancer, Cancer Biol. Ther. 21 (2020) 147–156, https://doi.org/10.1080/15384047.2019.1672455.

[102] Y. Gu, J. Zhang, H. Guan, Expression of EZH2 in endometrial carcinoma and its effects on proliferation and invasion of endometrial carcinoma cells, Oncol. Lett. 14 (2017) 7191–7196, https://doi.org/10.3892/ol.2017.7171.

[103] M.A. Quinn, et al., Correlation between cytoplasmic steroid receptors and tumour differentiation and invasion in endometrial carcinoma, Br. J. Obstet. Gynaecol. 92 (1985) 399–406, https://doi.org/10.1111/j.1471-0528.1985.tb01115.x.

[104] T. Fonnes, et al., Asparaginase-like protein 1 expression in curettage independently predicts lymph node metastasis in endometrial carcinoma: a multicentre study, BJOG 125 (2018) 1695–1703, https://doi.org/10.1111/1471-0528.15403.

[105] L. Vermij, et al., p53 immunohistochemistry in endometrial cancer: clinical and molecular correlates in the PORTEC-3 trial, Mod. Pathol. 35 (2022) 1475–1483, https://doi.org/10.1038/s41379-022-01102-x.

[106] M. Kobel, et al., Interpretation of P53 immunohistochemistry in endometrial carcinomas: toward increased reproducibility, Int. J. Gynecol. Pathol. 1 (2019) S123–S131, https://doi.org/10.1097/PGP.0000000000000488. **38 Suppl**.

[107] P.Y. Chu, Y.L. Tai, T.L. Shen, Grb7, a critical mediator of EGFR/ErbB signaling, in cancer development and as a potential therapeutic target, Cells 8 (2019), https://doi.org/10.3390/cells8050435.

[108] D. Stein, et al., The SH2 domain protein GRB-7 is co-amplified, overexpressed and in a tight complex with HER2 in breast cancer, EMBO J. 13 (1994) 1331–1340, https://doi.org/10.1002/j.1460-2075.1994.tb06386.x.

[109] A. Varis, et al., Targets of gene amplification and overexpression at 17q in gastric cancer, Cancer Res. 62 (2002) 2625–2629.

[110] Y. Nadler, et al., Growth factor receptor-bound protein-7 (Grb7) as a prognostic marker and therapeutic target in breast cancer, Ann. Oncol. 21 (2010) 466–473, https://doi.org/10.1093/annonc/mdp346.

[111] O. Giricz, et al., GRB7 is required for triple-negative breast cancer cell invasion and survival, Breast Cancer Res. Treat. 133 (2012) 607–615, https://doi.org/10.1007/s10549-011-1822-6.

[112] H. Tang, et al., Growth factor receptor bound protein-7 regulates proliferation, cell cycle, and mitochondrial apoptosis of thyroid cancer cells via MAPK/ERK signaling, Mol. Cell Biochem. 472 (2020) 209–218, https://doi.org/10.1007/s11010-020-03798-4.

[113] D.C. Han, T.L. Shen, H. Miao, B. Wang, J.L. Guan, EphB1 associates with Grb7 and regulates cell migration, J. Biol. Chem. 277 (2002) 45655–45661, https://doi.org/10.1074/jbc.M203165200.

[114] H. Li, et al., The adaptor Grb7 is a novel calmodulin-binding protein: functional implications of the interaction of calmodulin with Grb7, Oncogene 24 (2005) 4206–4219, https://doi.org/10.1038/sj.onc.1208591.

[115] S. Itoh, et al., Role of growth factor receptor bound protein 7 in hepatocellular carcinoma, Mol. Cancer Res. 5 (2007) 667–673, https://doi.org/10.1158/1541-7786.MCR-06-0282.

[116] S. Tanaka, et al., Grb7 signal transduction protein mediates metastatic progression of esophageal carcinoma, J. Cell. Physiol. 183 (2000) 411–415, https://doi.org/10.1002/(SICI)1097-4652(200006)183:3<411::AID-JCP14>3.0.CO;2-Z.

[117] S. Tanaka, et al., Specific peptide ligand for Grb7 signal transduction protein and pancreatic cancer metastasis, J. Natl. Cancer Inst. 98 (2006) 491–498, https://doi.org/10.1093/jnci/djj105.

[118] S.C. Pero, et al., Identification of novel non-phosphorylated ligands, which bind selectively to the SH2 domain of Grb7, J. Biol. Chem. 277 (2002) 11918–11926, https://doi.org/10.1074/jbc.M111816200.

[119] S.C. Pero, G.S. Shukla, M.M. Cookson, S. Flemer Jr., D.N. Krag, Combination treatment with Grb7 peptide and Doxorubicin or Trastuzumab (Herceptin) results in cooperative cell growth inhibition in breast cancer cells, Br. J. Cancer 96 (2007) 1520–1525, https://doi.org/10.1038/sj.bjc.6603732.

[120] H.K. Jensen, et al., Presence of intratumoral neutrophils is an independent prognostic factor in localized renal cell carcinoma, J. Clin. Oncol. 27 (2009) 4709–4717, https://doi.org/10.1200/JCO.2008.18.9498.

[121] D.M. Kuang, et al., Peritumoral neutrophils link inflammatory response to disease progression by fostering angiogenesis in hepatocellular carcinoma, J. Hepatol. 54 (2011) 948–955, https://doi.org/10.1016/j.jhep.2010.08.041.

[122] H.L. Rao, et al., Increased intratumoral neutrophil in colorectal carcinomas correlates closely with malignant phenotype and predicts patients' adverse prognosis, PLoS ONE 7 (2012) e30806, https://doi.org/10.1371/journal.pone.0030806.

[123] S. Trellakis, et al., Polymorphonuclear granulocytes in human head and neck cancer: enhanced inflammatory activity, modulation by cancer cells and expansion in advanced disease, Int. J. Cancer 129 (2011) 2183–2193, https://doi.org/10.1002/ijc.25892.

[124] J.J. Zhao, et al., The prognostic value of tumor-infiltrating neutrophils in gastric adenocarcinoma after resection, PLoS ONE 7 (2012) e33655, https://doi.org/10.1371/journal.pone.0033655.

[125] R.S. Berry, et al., High levels of tumor-associated neutrophils are associated with improved overall survival in patients with stage II colorectal cancer, PLoS ONE 12 (2017) e0188799, https://doi.org/10.1371/journal.pone.0188799.

[126] M.R. Galdiero, et al., Occurrence and significance of tumor-associated neutrophils in patients with colorectal cancer, Int. J. Cancer 139 (2016) 446–456, https://doi.org/10.1002/ijc.30076.

[127] A. Blaisdell, et al., Neutrophils oppose uterine epithelial carcinogenesis via debridement of hypoxic tumor cells, Cancer Cell 28 (2015) 785–799, https://doi.org/10.1016/j.ccell.2015.11.005.

[128] U. Batzorig, et al., The switch/sucrose nonfermentable subunit ARID1A mediates neutrophil-associated skin inflammatory responses, J. Investig. Dermatol. (2024), https://doi.org/10.1016/j.jid.2024.03.015.

[129] J.Z. Fang, et al., Hepatocyte-specific Arid1a deficiency initiates mouse steatohepatitis and hepatocellular carcinoma, PLoS ONE 10 (2015) e0143042, https://doi.org/10.1371/journal.pone.0143042.

[130] M. Feng, et al., Neutrophils as key regulators of tumor immunity that restrict immune checkpoint blockade in liver cancer, Cancer Biol. Med. 20 (2023) 421–437, https://doi.org/10.20892/j.issn.2095-3941.2023.0019.

[131] I. Di Ceglie, et al., Immune cell networking in solid tumors: focus on macrophages and neutrophils, Front. Immunol. 15 (2024) 1341390, https://doi.org/10.3389/fimmu.2024.1341390.

[132] A. Orlandi, et al., Cellular retinol binding protein-1 expression in endometrial hyperplasia and carcinoma: diagnostic and possible therapeutic implications, Mod. Pathol. 19 (2006) 797–803, https://doi.org/10.1038/modpathol.3800586.

[133] D.M. Badary, H. Abou-Taleb, Vitamin D receptor and cellular retinol-binding protein-1 immunohistochemical expression in normal, hyperplastic and neoplastic endometrium: possible diagnostic and therapeutic implications, Ann. Diagn. Pathol. 48 (2020) 151569, https://doi.org/10.1016/j.anndiagpath.2020.151569.

[134] M. Wilkinson, et al., The molecular effects of a high fat diet on endometrial tumour biology, Life (2020) 10, https://doi.org/10.3390/life10090188.

[135] D. Egan, et al., CRABP2–a novel biomarker for high-risk endometrial cancer, Gynecol. Oncol. 167 (2022) 314–322, https://doi.org/10.1016/j.ygyno.2022.09.020.

[136] Q. Lin, et al., Overexpression of nucleolin is a potential prognostic marker in endometrial carcinoma, Cancer Manag. Res. 13 (2021) 1955–1965, https://doi.org/10.2147/CMAR.S294035.
[137] V.D. Barzilova, et al., Role of nucleolin in endometrial precancerous hyperplasia and carcinogenesis: *ex vivo* and *in silico* study, Int. J. Mol. Sci. 23 (2022), https://doi.org/10.3390/ijms23116228.
[138] A. Darbandsari, et al., AI-based histopathology image analysis reveals a distinct subset of endometrial cancers, Nat. Commun. 15 (2024) 4973, https://doi.org/10.1038/s41467-024-49017-2.
[139] A. Jamieson, et al., Grade and estrogen receptor expression identify a subset of no specific molecular profile endometrial carcinomas at a very low risk of disease-specific death, Mod. Pathol. 36 (2023) 100085, https://doi.org/10.1016/j.modpat.2022.100085.
[140] L. Vermij, et al., Prognostic refinement of NSMP high-risk endometrial cancers using oestrogen receptor immunohistochemistry, Br. J. Cancer 128 (2023) 1360–1368, https://doi.org/10.1038/s41416-023-02141-0.
[141] M.M. Tajrishi, R. Tuteja, N. Tuteja, Nucleolin: the most abundant multifunctional phosphoprotein of nucleolus, Commun. Integr. Biol. 4 (2011) 267–275, https://doi.org/10.4161/cib.4.3.14884.
[142] W. Qiu, et al., The involvement of cell surface nucleolin in the initiation of CCR6 signaling in human hepatocellular carcinoma, Med. Oncol. 32 (2015) 75, https://doi.org/10.1007/s12032-015-0530-1.
[143] S. Yangngam, et al., Cellular localization of nucleolin determines the prognosis in cancers: a meta-analysis, J. Mol. Med. 100 (2022) 1145–1157, https://doi.org/10.1007/s00109-022-02228-w.
[144] S. Thongchot, K. Aksonnam, P. Thuwajit, P.T. Yenchitsomanus, C. Thuwajit, Nucleolin-based targeting strategies in cancer treatment: focus on cancer immunotherapy (Review), Int. J. Mol. Med. 52 (2023), https://doi.org/10.3892/ijmm.2023.5284.
[145] J. Balca-Silva, et al., Nucleolin is expressed in patient-derived samples and glioblastoma cells, enabling improved intracellular drug delivery and cytotoxicity, Exp. Cell Res. 370 (2018) 68–77, https://doi.org/10.1016/j.yexcr.2018.06.005.
[146] I. Winer, et al., F3-targeted cisplatin-hydrogel nanoparticles as an effective therapeutic that targets both murine and human ovarian tumor endothelial cells *in vivo*, Cancer Res. 70 (2010) 8674–8683, https://doi.org/10.1158/0008-5472.CAN-10-1917.
[147] J. Wu, et al., Nucleolin targeting AS1411 modified protein nanoparticle for antitumor drugs delivery, Mol. Pharm. 10 (2013) 3555–3563, https://doi.org/10.1021/mp300686g.
[148] S. Thongchot, et al., Adoptive transfer of anti-nucleolin T cells combined with PD-L1 inhibition against triple-negative breast cancer, Mol. Cancer Ther. 21 (2022) 727–739, https://doi.org/10.1158/1535-7163.MCT-21-0823.
[149] Y. Dou, et al., Proteogenomic insights suggest druggable pathways in endometrial carcinoma, Cancer Cell 41 (2023) 1586–1605, https://doi.org/10.1016/j.ccell.2023.07.007, e1515.